Fingering of exothermic reaction-diffusion fronts in Hele-Shaw cells with conducting walls

J. D'Hernoncourt[a)]
Service de Chimie Physique and Center for Nonlinear Phenomena and Complex Systems, CP 231, Université Libre de Bruxelles, 1050 Brussels, Belgium

S. Kalliadasis
Department of Chemical Engineering, Imperial College London, London SW7 2AZ, United Kingdom

A. De Wit[b)]
Service de Chimie Physique and Center for Nonlinear Phenomena and Complex Systems, CP 231, Université Libre de Bruxelles, 1050 Brussels, Belgium

(Received 2 August 2005; accepted 11 October 2005; published online 16 December 2005)

We consider the influence of heat losses through the walls of a Hele-Shaw cell on the linear stability and nonlinear dynamics of exothermic chemical fronts whose solutal and thermal contributions to density changes have the same signs. Our analysis is based on the reaction-diffusion-convection equations obtained from the Darcy-Boussinesq approximation. The parameters governing the equations are the Damköhler number, a kinetic parameter d, the Lewis number Le, the thermal-expansion coefficient γ_T, and a heat-transfer coefficient α which measures heat losses through the walls. We show that for thermally insulating walls, the temperature profile is a front that follows the concentration profile, while in the presence of heat losses, the temperature profile becomes a pulse that leads to a nonmonotonic density profile which in turn may lead to a destabilization of an otherwise stable front. © *2005 American Institute of Physics*.
[DOI: 10.1063/1.2136881]

I. INTRODUCTION

Density changes across a moving autocatalytic reaction-diffusion (RD) front traveling in the direction of gravity can induce a Rayleigh-Taylor instability if the heavier solution is placed on top of the lighter one in the gravity field.[1] Such a chemically induced hydrodynamic instability has been studied experimentally, first in capillary tubes[2–8] but also in Hele-Shaw cells (two glass plates separated by a thin gap width) allowing for easy visualization of the resulting density fingering of spatially extended fronts.[8–17] The total density jump $\Delta\rho$ across the front is a combination of solutal, $\Delta\rho_s$, and thermal, $\Delta\rho_T$, contributions. Depending on the relative partial molar volume of the reactants versus that of the products, the solutal contribution to density change across the front can be positive, $\Delta\rho_s>0$, which means that the products are heavier than the reactants, thus leading to unstable descending isothermal fronts. If, on the contrary, the reactants are heavier than the products, $\Delta\rho_s<0$, the isothermal fronts ascending in the gravity field feature cellular convection around the front. The thermal contribution to density change can also be of both signs with $\Delta\rho_T<0(>0)$ corresponding to exothermic (respectively, endothermic) reactions.

We can therefore classify all chemical fronts in essentially two categories depending on whether the solutal and thermal effects are cooperative (both $\Delta\rho_s$ and $\Delta\rho_T$ have the same sign) or antagonist ($\Delta\rho_s$ and $\Delta\rho_T$ have the opposite sign). The antagonist situation where the solutal and thermal effects are competing has long been recognized to lead to multicomponent convection and double-diffusive instabilities.[1,5] Both ascending and descending fronts can then finger depending on the relative strength of the two effects which can be tuned by varying the concentrations, gap width of the cell, or the thickness of the reactor walls. The influence of competing solutal and thermal effects on the appearance of the Rayleigh-Taylor and double-diffusive instabilities has been recently studied both theoretically[13,18] and experimentally[13,15] for the chlorite-tetrathionate (CT) reaction. It was shown that the exothermicity of the reaction can lead to destabilization of otherwise stable fronts and new types of fingering phenomena. The cooperative situation seems *a priori* to lead to simple convection only as solutal and thermal effects are reinforcing each other. It is therefore expected that for chemical fronts of this category, only ascending fronts corresponding to heavy and cold reactants on top of light and hot products, respectively, will be destabilized by density fingering (with endothermic autocatalytic reactions not reported up to date).

In this context, the purpose of our study is to analyze the influence of heat losses through the walls of the reactor on the linear stability of exothermic RD fronts. Indeed, theoretical approaches devoted to analyze the influence of heat effects on the fingering dynamics of chemical fronts (see Ref. 18 and references therein) have up to now typically assumed that the system is thermally insulated and the reactor operates adiabatically. Nevertheless, the experimental conditions can be quite different. Bazsa and co-workers have noted

[a)]Electronic mail: jdhernon@ulb.ac.be
[b)]Electronic mail: adewit@ulb.ac.be

quite a while ago that varying the rate at which the heat of reaction is dissipated through the walls of a capillary tube (by varying the outer diameter of the tube or the medium in which the tube is immersed) has a marked influence on the velocity of propagation of the front.[2,3] Experimental measurements of temperature profiles across a front also show that the maximum temperature difference across the front is less than the one expected from the heat of reaction ΔH due to heat losses through the walls.[6] More recently, differences in stability properties of CT fronts have been measured experimentally when heat losses through the plates of a Hele-Shaw cell are varied.[14] As the situation of antagonist solutal and thermal effects is already quite involved even for perfectly insulating walls,[14,18] we shall focus here on the simplest case of cooperative effects.

Thus our goal here is to analyze the density fingering of exothermic chemical fronts in the case where $\Delta\rho_s$ and $\Delta\rho_T$ have the same sign and, in particular, to investigate the influence of heat losses through the walls on the stability and nonlinear dynamics of the front. We shall focus on the case where both $\Delta\rho_s$ and $\Delta\rho_T$ are negative corresponding to a situation in which the products are lighter than the reactants and the reaction is exothermic (the reverse situation where $\Delta\rho_s$ and $\Delta\rho_T$ are both positive is a straighforward extension due to symmetry). This is the case, e.g., of the iodate-arsenous acid reaction, the fingering of which has been thoroughly analyzed both experimentally[4,7,9,10,17] and theoretically.[7,12,19–25]

We demonstrate that for thermally insulating walls, the temperature profile is a front that mimics the concentration profile; while in the presence of heat losses through the walls, the temperature profile becomes a pulse localized around the chemical front. This local heat production then leads to a nonmonotonic density profile which can profoundly modify the stability properties of the RD fronts. In particular, we show that conducting walls may lead to a destabilization of otherwise stable fronts.

The paper is organized as follows. In Sec. II, we present the model and the governing parameters of the system. In Sec. III, we construct the base state of the system and discuss the effect of the heat losses through the walls on the temperature and density profiles. In Sec. IV, we perform a linear stability analysis of the different base states and discuss the influence of the different parameters on the stability characteristic of the system. We analyze the nonlinear dynamics in Sec. V and a discussion and conclusions are given in Sec. VI.

II. MODEL

Our model system is a two-dimensional (2D) thin Hele-Shaw cell of length L_x and width L_y oriented vertically in the gravity field $\underline{g}$ (see Fig. 1). The gap width h of the cell is here assumed thin enough, $h \ll L_{x,y}$, so that the velocity field $\underline{u} = (u_x, u_y)$ of the incompressible flow is described by the 2D Darcy's law (2). The reaction is initiated at either the top or the bottom of the cell resulting in a descending or ascending front, respectively. The chemical traveling front we are focusing on is the solution of a reaction-diffusion-convection equation (4) for the concentration C of the solute that determines the density ρ of the solution [Eq. (3)]. The reaction triggers a temperature distribution also affecting ρ and governed by the energy balance in Eq. (5). This equation incorporates convection and diffusive transport terms, production by the reaction, and heat losses approximated by Newton's law of cooling $-\alpha(T-T_{\text{air}})$ where T_{air} is the temperature of the surrounding air (without loss of generality T_{air} is here set to zero) with α a composite heat-transfer coefficient that measures the rate of heat transfer from the liquid to the wall, through the wall, and from the wall to the surrounding air. The governing equations are

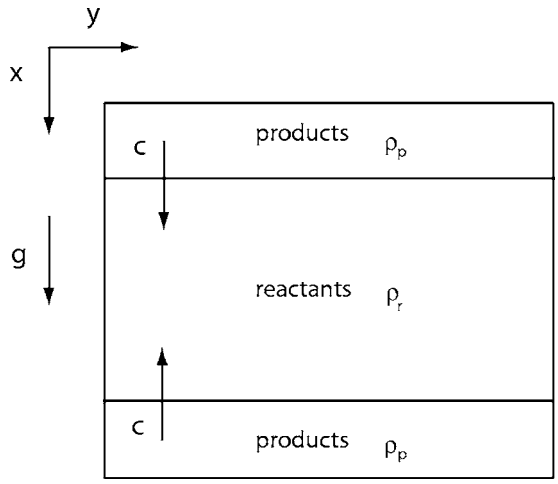

FIG. 1. Sketch of the system oriented vertically in the gravity field. The reaction is initiated either at the top or the bottom of the Hele-Shaw cell, resulting in downward or upward propagating fronts.

$$\underline{\nabla} \cdot \underline{u} = 0, \tag{1}$$

$$\underline{\nabla} p = -\frac{\mu}{K}\underline{u} + \rho(C,T)\underline{g}, \tag{2}$$

$$\rho = \rho_p + (\rho_r - \rho_p)\left(1 - \frac{C}{C_0}\right) + \gamma_T(T - T_0), \tag{3}$$

$$\frac{\partial C}{\partial t} + \underline{u} \cdot \underline{\nabla} C = D\nabla^2 C + f(C) \tag{4}$$

$$\rho_0 c_p \left[\frac{\partial T}{\partial t} + \underline{u} \cdot \underline{\nabla} T\right] = \kappa_T \nabla^2 T - \Delta H f(C) - \alpha T, \tag{5}$$

where p is the pressure and $K = h^2/12$ is the permeability of this model porous medium. The molecular diffusion coefficient D as well as the viscosity μ, the density ρ_0, the thermal conductivity κ_T, and the heat capacity c_p of water are here taken as constant. ΔH, the heat of the reaction, here is a negative quantity as the reaction is exothermic. As we also consider dilute solutions and temperature jumps of only a few degrees Kelvin across the front, the density is set to vary linearly with the concentration and the temperature and is given by (3) where ρ_r and ρ_p are the densities of the reactant and the product solutions, respectively. C_0 and T_0 are the initial concentration and temperature of the reactant while γ_T is the thermal-expansion coefficient. For (2) we have utilized the Boussinesq approximation assuming that small changes

in density are negligible except in the $\rho \underline{g}$ term of Darcy's equation. Note that Newton's law of cooling allows us to bypass the much more involved conjugated heat-transfer problem in the plate and the air (most of the resistance to heat transfer should be through the air due its low thermal conductivity compared to the liquid and the solid). Finally $f(C)$ is the dimensional kinetic term. As a model system we take here

$$f(C) = -(k_a + k_b C)C(C - C_0), \tag{6}$$

which is a quantitative model for the iodate-arsenous acid (IAA) reaction when arsenous acid is in excess[24,26] with $C_0 = [\mathrm{IO}_3^-]_0$ while k_a and k_b are kinetic constants.

Lengths, time, and velocities are nondimensionalized by the characteristic length $L = D/U$, time $\tau = D/U^2$, and speed $U = |\Delta\rho_s| gK/\nu$, where $\Delta\rho_s = (\rho_p - \rho_r)_s/\rho_r$ and $\nu = \mu/\rho_r$ is the kinematic viscosity. The pressure, density, and concentration are scaled by $\mu D/K$, $(\rho_r - \rho_p)_s$, and C_0, respectively, while the dimensionless temperature is defined from T/T_0. The dimensionless evolution equations are then

$$\underline{\nabla}' p' = -\underline{u}' + [\rho_p' + (1 - C') + \gamma_T' T']\underline{i}_x, \tag{7}$$

$$\underline{\nabla}' \cdot \underline{u}' = 0, \tag{8}$$

$$\frac{\partial C'}{\partial t'} + \underline{u}' \cdot \underline{\nabla}' C' = \nabla'^2 C' - \mathrm{Da} C'(C' - 1)(C' + d), \tag{9}$$

$$\frac{\partial T'}{\partial t'} + \underline{u}' \cdot \underline{\nabla}' T' = \mathrm{Le} \nabla'^2 T' - \phi \mathrm{Da} C'(C' - 1)(C' + d) - \alpha' T', \tag{10}$$

where the primes denote dimensionless variables. $d = k_a/k_b C_0$, $\alpha' = \alpha D/\rho_0 c_p U^2$, and $\gamma_T' = \gamma_T T_0/(\rho_r - \rho_p)_s \equiv \Delta\rho_T T_0/|\Delta\rho_s|\Delta T$, where ΔT is the adiabatic temperature rise and $\underline{i}_x$ is the unit vector in the x direction. The Damköhler number Da is defined as the ratio between the characteristic hydrodynamic time scale $\tau = D/U^2$ and the chemical time scale $\tau_c = 1/k_b C_0^2$. The Lewis number Le is defined as the ratio between the thermal diffusivity $D_T = \kappa_T/\rho_0 c_p$ and the molecular diffusivity D. The parameter ϕ is the exothermicity of the system defined as $\phi = |\Delta H| C_0/\rho_0 c_p T_0$.

We next define a new hydrostatic pressure gradient from $\underline{\nabla}' p'' = \underline{\nabla}' p' - (\rho_p' - \gamma_T')\underline{i}_x$, while the temperature and the dimensionless expansion coefficient are redefined as $T'' = T'/\phi$ and $\gamma_T'' = \phi\gamma_T'$, thus scaling away ϕ from the energy equation. After dropping the primes, (7)–(11) become

$$\underline{\nabla} p = -\underline{u} + [(1 - C) + \gamma_T T]\underline{i}_x, \tag{11}$$

$$\underline{\nabla} \cdot \underline{u} = 0, \tag{12}$$

$$\frac{\partial C}{\partial t} + \underline{u} \cdot \underline{\nabla} C = \nabla^2 C - \mathrm{Da} C(C - 1)(C + d), \tag{13}$$

$$\frac{\partial T}{\partial t} + \underline{u} \cdot \underline{\nabla} T = \mathrm{Le} \nabla^2 T - \mathrm{Da} C(C - 1)(C + d) - \alpha T. \tag{14}$$

Notice that for $\gamma_T = 0$, Eqs. (11)–(13) are decoupled from the heat equation (14). We then recover in this limit the isothermal density fingering of the IAA reaction studied in detail for the same dimensionless system in Refs. 24 and 25.

III. TRAVELING FRONTS

We now construct the one-dimensional (1D) base state of our system both with and without heat losses. In the absence of convection, the concentration and temperature profiles are the solutions of the system,

$$\frac{\partial C}{\partial t} = \frac{\partial^2 C}{\partial x^2} - \mathrm{Da} C(C - 1)(C + d), \tag{15}$$

$$\frac{\partial T}{\partial t} = \mathrm{Le} \frac{\partial^2 T}{\partial x^2} - \mathrm{Da} C(C - 1)(C + d) - \alpha T. \tag{16}$$

The $C = 1$ solution is the stable chemical steady state of the cubic kinetics corresponding to the products of the reaction, while $C = 0$ is the unstable state corresponding to the reactants.

A. Concentration fronts

The 1D stable steady state invades the unstable one giving rise to a planar front. The analytical solution of Eq. (15) is[26]

$$C(x,t) = \frac{1}{2}\left[1 + \tanh \frac{1}{2}\sqrt{\frac{\mathrm{Da}}{2}}(x \pm vt)\right] = \frac{1}{1 + e^{-\sqrt{\mathrm{Da}/2}(x \pm vt)}}, \tag{17}$$

where the signs + and − correspond to the ascending and descending fronts, respectively. The reaction front travels with a speed $v = \sqrt{\mathrm{Da}/2}(1 + 2d)$ and has a width w, defined as the distance between $C = \delta$ and $C = 1 - \delta$, which is equal to $w = \sqrt{8/\mathrm{Da}} \ln[(1 - \delta)/\delta]$. Thus increasing Da leads to sharper fronts traveling faster.

Note that as was shown by Ben-Jacob *et al.*,[27] the above solution is the dynamically selected front only for $d < 1.2$. For other values of d the selected front becomes a Fisher front traveling at velocity $2\sqrt{\mathrm{Da}}$.

B. Thermal fronts

If the reaction is exothermic, the concentration front (17) generates a heat front as well with a speed determined by the concentration profile. This front can be obtained analytically from (16) but the functional form is cumbersome as it involves integrals of various combinations of (17) that have to be obtained numerically as they cannot be formulated in terms of known functions. We thus obtain the temperature profiles as a function of the two parameters Le and α by integrating Eqs. (15) and (16) numerically as an initial value problem. The numerical scheme is based on a fourth-order Runge-Kutta scheme for the temporal derivatives and a finite differencing scheme for the spatial derivatives. We impose no-flux boundary conditions, $C_x, T_x \to 0$ as $x \to \pm\infty$, while the

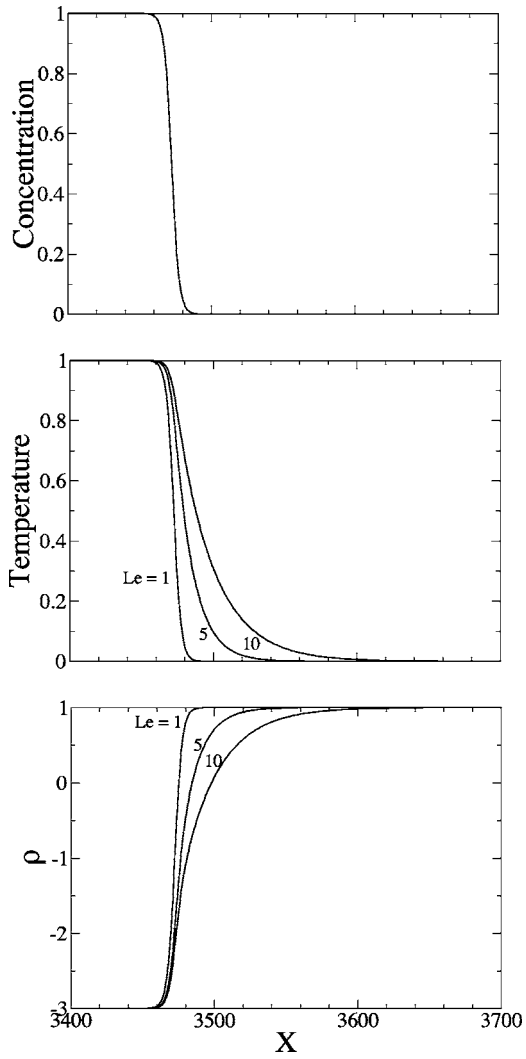

FIG. 2. Concentration, temperature, and density profiles in the case of insulating walls ($\gamma_T=-3$, $\alpha=0$) for different values of the Lewis number Le.

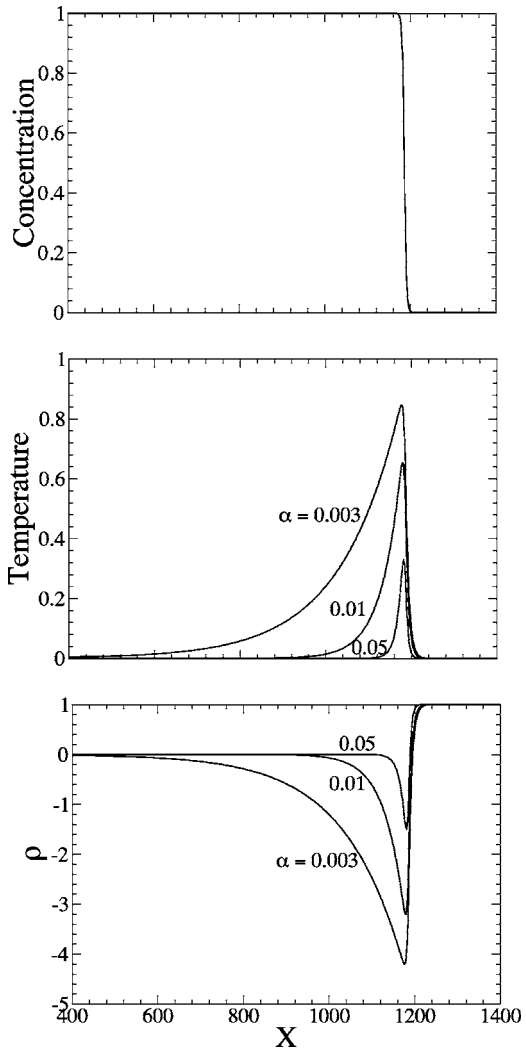

FIG. 3. Concentration, temperature, and density profiles ($\gamma_T=-5$, Le=3) for different values of the cooling coefficient α.

initial condition for both T and C is chosen to be either a step function or the solution (15). The profiles presented here are the asymptotic ones for large t.

We fix throughout this article the kinetic parameter to $d=0.01$ and the Damköhler number to Da=0.3, typical values for which several results have already been obtained in the case of isothermal systems.[24,25] We then examine the influence of the two parameters Le and α on the form of the thermal fronts. When $\alpha=0$, i.e., for perfectly insulating walls, all the heat produced by the chemical reaction is kept inside the reactor. This is the adiabatic limit. The solutions of the system (15) and (16) then give thermal traveling fronts connecting the temperature $T=0$ of the reactants (cold) to the temperature $T=1$ of the products (hot). If Le=1, mass and heat diffuse at the same rate and the thermal front is then exactly the same as the concentration one given by the solution (17). For increasing values of Le, heat diffuses faster than the mass and the thermal front becomes wider than the chemical front (Fig. 2). We thus have a monotonic temperature profile that connects the hot products to the cold reactants. As a consequence, the density profile $\rho(x)=1-C(x)+\gamma_T T(x)$ is also monotonic between the density of the reactants $\rho_r=1$ (for $C=0$, $T=0$) and that of the products $\rho_p=\gamma_T$ (for $C=1$, $T=1$). For an exothermic reaction ($\gamma_T<0$), the total density jump $\Delta\rho=\rho_p-\rho_r=\gamma_T-1$ is always larger than the isothermal contribution $\Delta\rho_s=-1$. Let us note that, with such monotonous density profiles, the typical buoyantly unstable situation is that of ascending fronts for which heavy and cold reactants are lying on top of light and hot products. The descending situation, on the contrary, is expected to be stable.

In the case of conducting walls, $\alpha\neq 0$, the temperature profiles are no longer traveling fronts but traveling pulses as shown in Fig. 3. For a fixed location in space and when a chemical front passes by, we see successively a zone of cold reactants, a zone of hot products, and finally a region of products that have cooled down because heat losses have partially dissipated the heat of the products towards the surroundings. The amplitude and spatial extent of the heat pulse is a function of both Le and α. This nonmonotonous temperature distribution gives rise to a nonmonotonous density profile which can trigger the onset of unstable density stratifications for descending fronts as well. Indeed, in that case, the presence of cold products on top of hot products inside

the front is a potentially unstable situation with regards to the Rayleigh-Taylor instability. This intuitive argument will now be examined quantitatively with the means of a linear stability analysis.

IV. LINEAR STABILITY

We now analyze the stability of the fronts characterized in the previous section with regards to infinitesimal hydrodynamic perturbations in the transverse direction.

A. Eigenvalue problem

Introducing the Lagrangian coordinate $z=x+vt$ to examine the evolution of infinitesimal disturbances in a frame moving with the reaction-diffusion velocity v, the base state of Eqs. (11)–(14) is given by

$$\underline{u}=\underline{u}_s=0, \quad C=C_s(z), \quad T=T_s(z), \quad p=p_s(z),$$

where $C_s(z)$ and $T_s(z)$ are the analytic solution (17) and the temperature profile determined numerically in the previous section, respectively. Once these profiles are known, the pressure distribution can be readily obtained from

$$\frac{dp_s}{dz}=(1-C_s)+\gamma_T T_s. \tag{18}$$

The pressure is indeed only a function of z as $dp/dy=-u_{ys}=0$ with u_{ys} the fluid velocity in the y direction. Let us then write $\underline{u}=\underline{u}_s+\underline{u}_1$, $C=C_s(z)+C_1$, $T=T_s(z)+T_1$, and $p=p_s(z)+p_1$ with $\underline{u}_1$, C_1, T_1, and p_1 being small perturbations. Inserting these expressions into (11)–(14) and linearizing the resulting equations, we get the evolution equations for the disturbances:

$$\frac{\partial p_1}{\partial z}=-u_{1z}-(C_1-\gamma_T T_1), \tag{19}$$

$$\frac{\partial p_1}{\partial y}=-u_{1y}, \tag{20}$$

$$\frac{\partial C_1}{\partial t}+v\frac{\partial C_1}{\partial z}+u_{1z}\frac{\partial C_s}{\partial z}=\frac{\partial^2 C_1}{\partial z^2}+\frac{\partial^2 C_1}{\partial y^2}+\mathrm{Da}\left.\frac{df}{dC}\right|_{C_s} C_1, \tag{21}$$

$$\frac{\partial T_1}{\partial t}+v\frac{\partial T_1}{\partial z}+u_{1z}\frac{\partial T_s}{\partial z}=\mathrm{Le}\frac{\partial^2 T_1}{\partial z^2}+\mathrm{Le}\frac{\partial^2 T_1}{\partial y^2}+\mathrm{Da}\left.\frac{df}{dC}\right|_{C_s} C_1-\alpha T_1, \tag{22}$$

$$\frac{\partial u_{1z}}{\partial z}+\frac{\partial u_{1y}}{\partial y}=0. \tag{23}$$

We now seek solutions of Eqs. (19)–(23) in the form of normal modes:

$$(u_{1z},u_{1y},p_1,C_1,T_1)=(\bar{u}_z(z),\bar{u}_y(z),\bar{p}(z),\bar{C}(z),\bar{T}(z))e^{\sigma t+iky}+\text{c.c.}, \tag{24}$$

where σ is the growth rate of the perturbations and k their wave number. This leads to the following eigenvalue problem for $(\bar{u}_z,\bar{u}_y,\bar{p},\bar{C},\bar{T})$ in terms of the growth rate σ:

$$\frac{d\bar{p}}{dz}=-\bar{u}_z-(\bar{C}-\gamma_T\bar{T}), \tag{25}$$

$$ik\bar{p}=-\bar{u}_y, \tag{26}$$

$$\sigma\bar{C}+v\frac{d\bar{C}}{dz}+\bar{u}_z\frac{dC_s}{dz}=\frac{d^2\bar{C}}{dz^2}-k^2\bar{C}+\mathrm{Da}\left.\frac{df}{dC}\right|_{C_s}\bar{C}, \tag{27}$$

$$\sigma\bar{T}+v\frac{d\bar{T}}{dz}+\bar{u}_z\frac{dT_s}{dz}=\mathrm{Le}\frac{d^2\bar{T}}{dz^2}-\mathrm{Le}k^2\bar{T}+\mathrm{Da}\left.\frac{df}{dT}\right|_{C_s}\bar{C}-\alpha\bar{T}, \tag{28}$$

$$\frac{d\bar{u}_z}{dz}+ik\bar{u}_y=0, \tag{29}$$

subject to the boundary conditions that the perturbations vanish far away from the front,

$$\bar{C},\bar{T},\bar{u}\to 0 \quad \text{when } z\to\pm\infty,$$

so that we restrict our attention to eigenfunctions that decay to zero at the infinities and correspond to disturbances localized around the reaction-diffusion front. This eigenvalue problem is solved using the technique described in Refs. 18 and 28. The method involves the discretization of Eqs. (25)–(29) using a second-order finite differencing scheme. The differential eigenvalue problem is then converted to a matrix eigenvalue problem of the form

$$\underline{\underline{M}}\begin{bmatrix}\underline{C}\\ \underline{T}\end{bmatrix}=\sigma\begin{bmatrix}\underline{C}\\ \underline{T}\end{bmatrix}. \tag{30}$$

The problem is solved numerically using a LAPACK solver to obtain the growth rate σ of the disturbances as a function of their wave number k. We tested the accuracy of the method by varying the mesh and the domain size until no changes occurred in the dispersion curves. The numerical code recovers the same dispersion curves as those previously analyzed for the isothermal IAA case.[24] Moreover it reproduces the exothermic curves obtained for the CT exothermic fronts analyzed in Ref. 18.

B. Dispersion curves

To analyze the influence of heat effects on the stability of chemical fronts with regards to fingering, we fix again the kinetic parameter to $d=0.01$ and the Damköhler number to $\mathrm{Da}=0.3$. The three other characteristic parameters of the thermal effects, i.e., the Lewis number Le, the thermal-expansion coefficient γ_T, and the dimensionless heat-transfer coefficient α are varied successively.

Let us first focus on the ascending fronts which are genuinely unstable for isothermal conditions ($\gamma_T=0$). Indeed, we analyze here a situation for which the solutal contribution to density decreases in the course of the reaction ($\Delta\rho_s<0$)

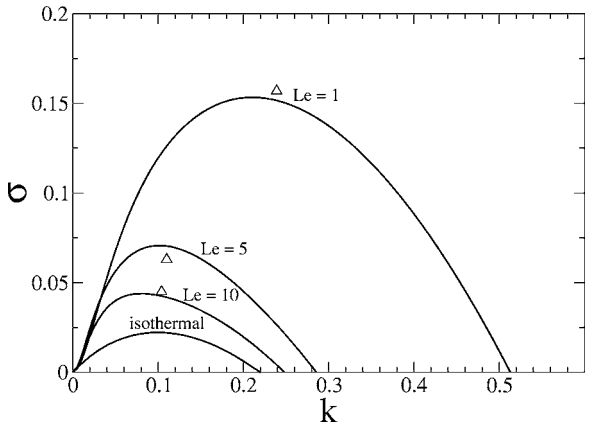

FIG. 4. Dispersion curves giving the growth rate σ of the perturbations as a function of the wave number k of ascending fronts for different values of the Lewis number Le ($\gamma_T=-3$, $\alpha=0$). The triangles denote the values of the most unstable wave number observed at short times in the nonlinear simulations.

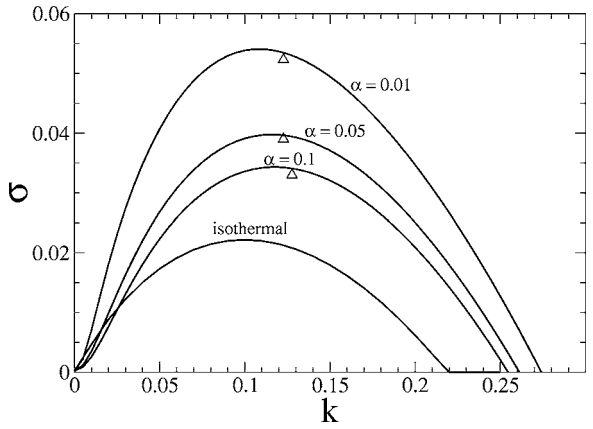

FIG. 5. Dispersion curves for ascending fronts and different values of Newton's cooling coefficient α (Le=5, $\gamma_T=-3$). The triangles denote the values of the most unstable wave number observed at short times in the nonlinear simulations.

thus leading to heavier reactants lying on top of lighter products, a buoyantly unstable stratification. If the reaction is exothermic, the effect of the temperature rise across the front is to increase the density jump ($\Delta\rho_T<0$) between the cold and heavy reactants and the hot and light products. Thus, by increasing the magnitude of the total density jump $\Delta\rho$, the exothermicity of the reaction can only lead to more unstable ascending fronts. Nevertheless, the thermal contribution depends strongly on the Lewis number Le. Figure 4 shows the dispersion curves featuring the growth rate σ of the perturbations as a function of their wave number k for different values of the Lewis number for $\gamma_T=-3$ and insulating walls ($\alpha=0$). When Le is increased, the system becomes more stable which can be understood as, for larger Le, the temperature profile is more spatially spread out leading to a smaller density gradient (the same density jump acts on a more spatially extended zone). As a consequence when Le increases the amount of heat diffusing from the hot products to the cold reactants increases thus making the products cooler and hence heavier. When $\mathrm{Le}\to\infty$, we recover the isothermal situation.

Let us now examine the influence of heat losses through the walls. Figure 5 shows the dispersion curves for Le=5, $\gamma_T=-3$ and different values of the dimensionless heat-transfer coefficient α. Obviously, dissipation of heat out of the reactor leaves less heat inside the system and the fronts are thus more stable than in the case of perfectly insulating walls. When $\alpha\to\infty$, all the heat produced by the reaction escapes from the system and the dispersion curve of the isothermal system is recovered in this limit. All dispersion curves for ascending fronts feature a band of unstable modes extending from $k=0$ up to a cutoff wave number k_c above which the system is linearly stable. This unstable band $0<k<k_c$ contains the wave number $k_{\max}$ with maximum growth rate $\sigma_{\max}$. Notice the weak dependence of the maximum growing wave number on α. These dispersion curves are similar to those of the pure Rayleigh-Taylor density fingering.[18,24]

We now turn to the descending fronts. In the case of insulating walls, the downward propagating front is observed to be stable as the density stratification with hot and light products on top of cold and heavy reactants is a statically stable situation. As anticipated from the density profiles discussed in the previous section, conducting walls with $\alpha\neq 0$ lead for the case of downward propagating fronts to a locally unstable density stratification of cooled products overlying hot ones. The linear stability analysis gives in this case dispersion curves that are dramatically different from the ones for the up going fronts as they are characterized by a band of unstable modes with $k_1<k<k_2$ centered around the most unstable wave number with the band $0<k<k_1$ being stable (see Fig. 6). These dispersion curves are reminiscent of the Turing-type instabilities for which a critical value of a parameter has to be crossed for the instability to set in and which results in a stationary pattern of constant wavelength. Figure 6 and the related profiles of Fig. 3 allow to understand that for large heat losses (here typically $\alpha=0.05$), we are close to the isothermal case which is a stable density stratification for the downward moving fronts. Hence the growth rates are negative. For intermediate values of α, the extent of the region of hot products lying below the cooled products is large enough and the density jump across it is high enough

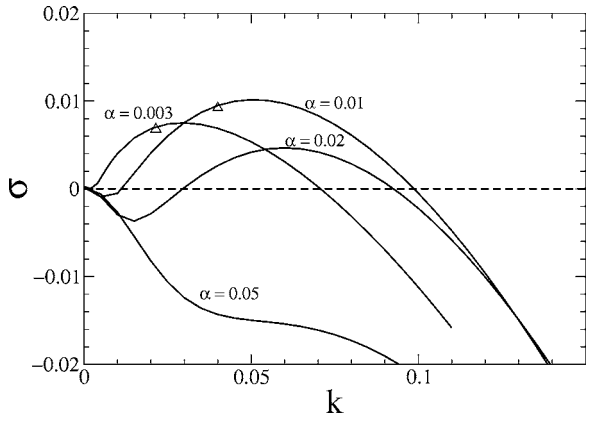

FIG. 6. Dispersion curves for descending fronts and different values of Newton's cooling coefficient α (Le=3, $\gamma_T=-5$). The triangles denote the values of the most unstable wave number observed at short times in the nonlinear simulations.

for a destabilization of a given band of wave numbers to be observed. For still smaller values of α (typically for $\alpha = 0.003$), the spreading of the pulse increases and the gradient of density decreases leading to a smaller destabilization than for intermediate values of α. This translates to the dispersion relation by the decrease of the maximum growth rate. For $\alpha \to 0$, the gradient of density behind the front is so small that we recover the stable descending front of the insulating case. Eventually, we note that, for a fixed α, increasing Le leads to a more extended pulse and hence destabilization of descending fronts but stabilization of ascending fronts. Let us now test the predictions of this linear stability analysis with an integration of the fully nonlinear model.

V. NONLINEAR RESULTS

In this section we analyze the nonlinear dynamics of the exothermic reaction-diffusion front subject to a Rayleigh-Taylor instability in the case of both insulating and conducting walls. To do so, we consider the full nonlinear model of Eqs. (11)–(14). We introduce the stream function ψ in the usual way so that $u_x = \partial_y \psi$ and $u_y = -\partial_x \psi$. Taking the curl of (11) we get the system

$$\nabla^2 \psi = -\partial_y C + \gamma_T \partial_y T, \tag{31}$$

$$\frac{\partial C}{\partial t} + \partial_x C \partial_y \psi - \partial_y C \partial_x \psi = \nabla^2 C - \mathrm{Da} C(C-1)(C+d), \tag{32}$$

$$\frac{\partial T}{\partial t} + \partial_x T \partial_y \psi - \partial_y T \partial_x \psi = \mathrm{Le} \nabla^2 T - \mathrm{Da} C(C-1)(C+d) - \alpha T, \tag{33}$$

where the subscripts x and y denote partial derivatives with regard to space. To solve this system numerically we use a pseudospectral scheme developed by Tan and Homsy[29] modified to take the chemistry and the thermal effects into account.[18,25,28,30] The program is based on the Fourier expansions of the stream function ψ, the concentration C, and the temperature T. We integrate the system in a two-dimensional domain of dimensionless width $L'_y = \Delta\rho_s g K L_y / \nu D$ (which is, in fact, the Rayleigh number Ra of our problem) and length $L'_x = \Delta\rho_s g K L_x / \nu D$. The simulations are started using a step function for both C and T. The reaction is initiated at the same time at both the top and the bottom of the reactor allowing us to follow simultaneously the dynamics of both the downward and upward propagating fronts. The concentration C is plotted in a scale of grey ranging from $C=0$ (white) to $C=1$ (black). We have first tested that our nonlinear simulations correctly reproduce the predictions of the linear stability analysis. As can be seen on the dispersion curves of Figs. 4–6 obtained for various values of the parameters, the main characteristics of the fingers appearing at onset in laterally extended systems, namely, maximum growing wave number and growth rate, and represented there as triangles are in good agreement with those predicted by the linear stability analysis.

In the nonlinear stage for the case of insulating walls (Fig. 7), we observe that the descending front remains stable while a rapid merging and coarsening of the fingers leads to the emergence of one single finger traveling with a constant shape and speed. This trend is similar to the one observed numerically for isothermal IAA ascending fronts.[23,25] For the conducting walls, i.e., $\alpha \neq 0$, we see that, indeed, the downward propagating front is unstable featuring low amplitude frozen fingers of constant amplitude and wavelength (Fig. 8). This is related to the fact that the instability inside the pulse is subdued by a region of stability below the front where the hot products meet the cool reactants. Hence the fingers cannot really develop as in the standard Rayleigh-Taylor instabilities. This is coherent with the fact that the corresponding dispersion curves witness a fixed band of unstable modes with the long-wave modes being stable. This has already been shown previously to freeze the pattern and inhibit coarsening.[18] For the upward propagating front the asymptotic dynamics of the finger is totally different with the heat losses through the walls leading to enhanced tip splitting (Fig. 8).

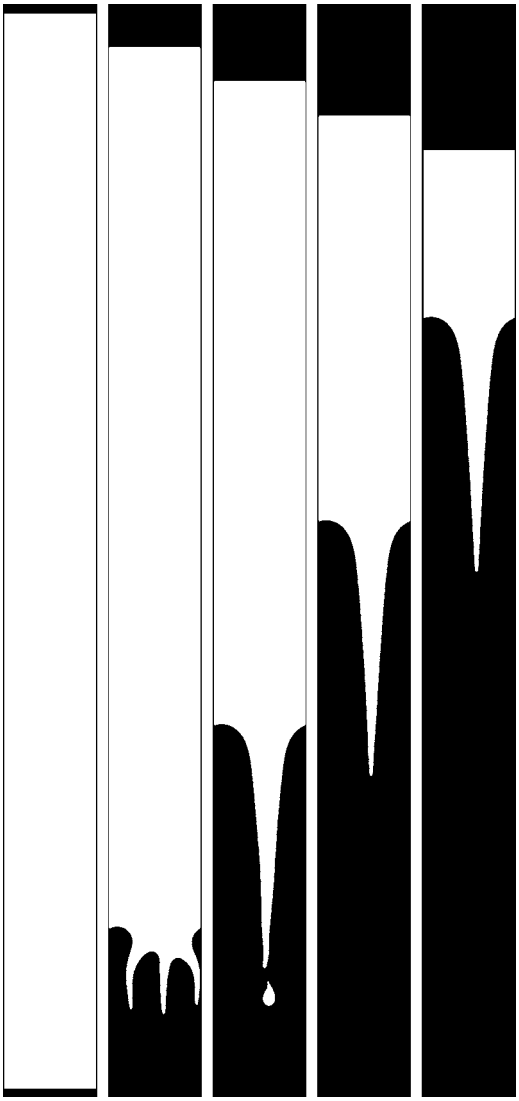

FIG. 7. Nonlinear dynamics of fingering of exothermic reaction-diffusion fronts in the case of insulating walls ($\alpha=0$) for the parameters Le=3 and $\gamma_T=-5$. The time interval between two images is 500 units of time. The width of the integration domain is 512. The descending front is stable while the ascending one features coarsening towards one single finger traveling with constant shape and speed.

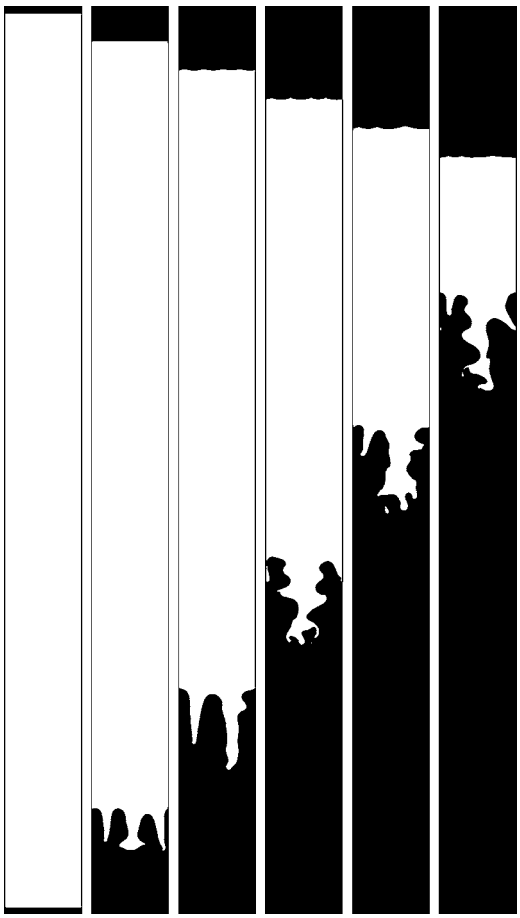

FIG. 8. Nonlinear dynamics of fingering of exothermic reaction-diffusion fronts in the case of conducting walls for the same parameters as in Fig. 7 except $\alpha=0.01$. The descending front is unstable as witnessed by the small modulation of the interface. The ascending front features very strong tip splittings.

VI. DISCUSSION

We have examined the influence of heat losses through the walls of a Hele-Shaw reactor on the fingering instability of a RD front for which the thermal and solutal contributions to the density jump across the front are cooperative so that both decrease the density during the reaction. In this case, it is expected that only ascending fronts are unstable as they correspond to a stratification of heavy and cold reactants on top of light and hot products. In insulated reactors and in the absence of convection, both concentration and temperature profiles are traveling fronts connecting the hot products to the cold reactants. If, on the contrary, the heat produced by the reaction is partially lost trough the plates, the temperature profile is no longer a front but a pulse of heat. We have performed the linear stability analysis of these fronts and pulses with respect to transverse buoyancy-driven instabilities. We have obtained the dispersion relations for the growth rate of these perturbations as a function of their wave number for various values of the important thermal parameters of the problem which are the Lewis number Le, the thermal-expansion coefficient γ_T, and the dimensionless heat-transfer coefficient α in Newton's law of cooling.

We have analyzed the influence of Le and α on the stability of the upward propagating front. It was shown that the dispersion curves in this case are similar to the classical curves found in the case of fingering of the isothermal IAA reaction. Moreover, the unstable system for perfectly insulating walls can be stabilized by the heat losses. For descending fronts, heat losses can, on the contrary, be a source of destabilization because of the nonmonotonicity of the density profile induced by the existence of the heat pulse localized around the front. Destabilization then occurs because of the local stratification of cooled products behind the front on top of hot products inside the front. The corresponding dispersion curves feature a finite band of unstable modes as in the Turing-type instabilities, i.e., long-waves modes are now stabilized on the contrary to the case of ascending fronts. Numerical integration of the fully nonlinear model for both upward and downward propagating fronts confirm the predictions of the linear stability analysis providing at onset fingers with the wavelength predicted. The nonlinear dynamics in the case of insulating walls feature coarsening of the ascending fingers towards one single finger propagating at a speed greater than the reaction-diffusion one just as observed in isothermal systems.[23,25] The situation is dramatically different for conducting walls. In that case, we observe enhanced tip splittings for ascending fronts and confirm the possibility of destabilization of descending fronts which appear as slight convective modulations of the interface.

Our results call for a careful inspection and analysis of future experimental results on the stability and nonlinear dynamics of exothermic chemical fronts. Obviously, heat losses through the walls have a quantitative influence on dispersion curves and on the occurrence of tip splittings, but even more drastically they can lead to the destabilization of fronts that would be stable in insulated systems. The fact that, in experiments, tip splittings are genuinely observed for ascending IAA fronts[17] calls for a check of the influence of heat losses on this dynamics. In particular, numerical simulations of the asymptotic nonlinear dynamics of ascending isothermal IAA fronts have shown an evolution towards one single finger featuring self-similar properties for Ra below a critical value Ra_c.[25] Above this Ra_c, tip splittings come into play. Here, we observe that for insulated walls, we also get one asymptotic finger while numerous splitting events come into play for the same values of parameters but conducting walls. It would be interesting, for example, to check whether the single finger obtained here for an exothermic reaction features self-similar properties analogous to those of isothermal systems.[25,30] Similarly, comparison between the rate of tip splitting events with or without heat losses would be worth undertaken. In another perspective, nonhomogeneous distribution of heat losses produced by cooling locally parts of the walls could also be used to control the fingering pattern as has been demonstrated in other systems.[31]

ACKNOWLEDGMENTS

One of the authors (J.D.) is supported by a FRIA (Belgium) Ph.D. fellowship. Another author (A.D.) acknowledges Prodex (Belgium) and the Communauté Française de Belgique (Actions de Recherches Concertées Programme) for the financial support. Another author (S.K.) thanks the

Center for Nonlinear Phenomena and Complex Systems, Université Libre de Bruxelles for their hospitality.

[1] J. A. Pojman and I. R. Epstein, J. Phys. Chem. **94**, 4966 (1990).
[2] G. Bazsa and I. R. Epstein, J. Phys. Chem. **89**, 3050 (1985).
[3] I. Nagypal, G. Bazsa, and I. R. Epstein, J. Am. Chem. Soc. **108**, 3635 (1986).
[4] J. A. Pojman, I. R. Epstein, T. J. McManus, and K. Showalter, J. Phys. Chem. **95**, 1299 (1991).
[5] J. A. Pojman, I. P. Nagy, and I. R. Epstein, J. Phys. Chem. **95**, 1306 (1991).
[6] I. P. Nagy and J. A. Pojman, J. Phys. Chem. **97**, 3443 (1993).
[7] J. Masere, D. A. Vasquez, B. F. Edwards, J. W. Wilder, and K. Showalter, J. Phys. Chem. **98**, 6505 (1994).
[8] I. P. Nagy, A. Keresztessy, J. A. Pojman, G. Bazsa, and Z. Noszticzius, J. Phys. Chem. **98**, 6030 (1994).
[9] M. R. Carey, S. W. Morris, and P. Kolodner, Phys. Rev. E **53**, 6012 (1996).
[10] M. Böckmann and S. C. Müller, Phys. Rev. Lett. **85**, 2506 (2000).
[11] D. Horváth, T. Bánsági, Jr., and A. Tóth, J. Chem. Phys. **117**, 4399 (2002).
[12] J. Martin, N. Rakotomalala, D. Salin, and M. Böckmann, Phys. Rev. E **65**, 051605 (2002).
[13] T. Bánsági, Jr., D. Horváth, Á. Tóth, J. Yang, S. Kalliadasis, and A. De Wit, Phys. Rev. E **68**, 055301 (2003).
[14] T. Bánsági, Jr., D. Horváth, and Á. Tóth, Phys. Rev. E **68**, 026303 (2003).
[15] T. Bánsági, Jr., D. Horváth, and Á. Tóth, Chem. Phys. Lett. **384**, 153 (2004).
[16] T. Bánsági, Jr., D. Horváth, and Á. Tóth, J. Chem. Phys. **121**, 11912 (2004).
[17] M. Böckmann and S. C. Müller, Phys. Rev. E **70**, 046302 (2004).
[18] S. Kalliadasis, J. Yang, and A. De Wit, Phys. Fluids **16**, 1395 (2004).
[19] D. A. Vasquez, J. W. Wilder, and B. F. Edwards, J. Chem. Phys. **98**, 2138 (1993).
[20] D. A. Vasquez, J. M. Littley, J. W. Wilder, and B. F. Edwards, Phys. Rev. E **50**, 280 (1994).
[21] Y. Wu, D. A. Vasquez, J. W. Wilder, and B. F. Edwards, Phys. Rev. E **52**, 6175 (1995).
[22] D. A. Vasquez, J. W. Wilder, and B. F. Edwards, J. Chem. Phys. **104**, 9926 (1996).
[23] J. Huang and B. F. Edwards, Phys. Rev. E **54**, 2620 (1996).
[24] A. De Wit, Phys. Rev. Lett. **87**, 054502 (2001).
[25] A. De Wit, Phys. Fluids **16**, 163 (2004).
[26] A. Saul and K. Showalter, in *Oscillations and Traveling Waves in Chemical Systems*, edited by R. J. Field and M. Burger (Wiley, New York, 1985).
[27] E. Ben-Jacob, H. Brand, G. Dee, L. Kramer, and J. S. Langer, Physica D **14**, 348 (1985).
[28] J. Yang, A. D'Onofrio, S. Kalliadasis, and A. De Wit, J. Chem. Phys. **117**, 9395 (2002).
[29] C. T. Tan and G. M. Homsy, Phys. Fluids **31**, 1330 (1988).
[30] D. Lima, A. D'Onofrio, and A. De Wit, J. Chem. Phys. (in press).
[31] D. A. Bratsun, Y. Shi, K. Eckert, and A. De Wit, Europhys. Lett. **69**, 746 (2005).